

Transition from Schottky to Ohmic Contacts in C₃₁ and MoS₂ van der Waals heterostructure

Lijun Xu, Guohui Zhan, Kun Luo, Fei Lu, Shengli Zhang and Zhenhua Wu*

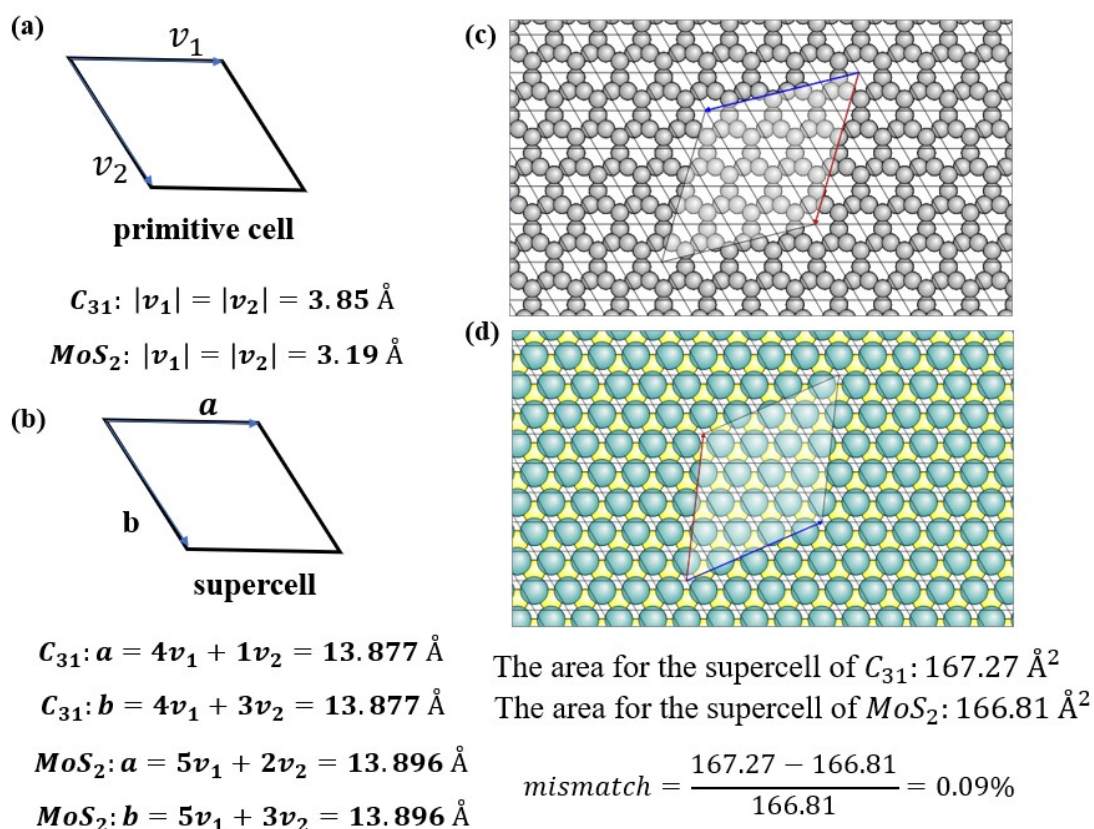


Fig. S1: The schematic diagram of primitive cell (a) and supercell (b). (c) and (d) are supercells of C_{31} and MoS_2 .

Fig. S1(a) displays the fundamental arrangement and lattice dimensions of the primitive cell, while Fig. S1(b) depicts the process of constructing the supercell. The configurations of C_{31} and MoS_2 can be observed in Figures S1(c) and S1(d), respectively. The MoS_2 supercell remains unaltered, whereas all strain is applied to the C_{31} supercell. The mismatch is estimated by comparing the areas of their supercells, as demonstrated in Fig. S1(d).

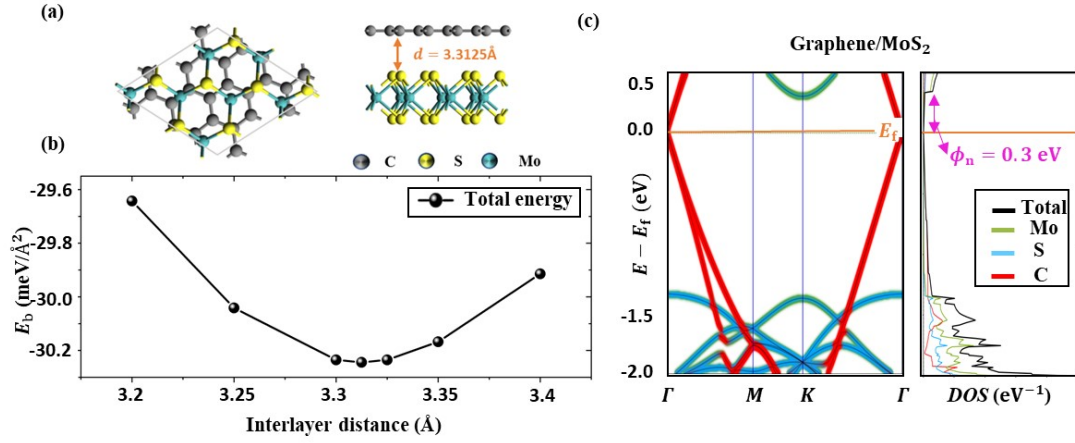


Fig. S2: (a) Top and side views of Graphene/MoS₂ heterostructure, and the interlayer distance is 3.3125 Å. The mismatch of Graphene/MoS₂ heterostructure is 0.18%. (b) The dependence of the binding energy on the interlayer distance, the minimum of binding energy is obtained at Interlayer distance = 3.3125 Å. (c) Weighted band structure and density of states (DOS) of heterostructure with the green blue and red colors indicating the contribution of molybdenum (Mo), carbon (C), and sulfur (S) elements, respectively.

Table: S1

The changes in lattice structure and Schottky barrier height as well as the bandgap of the semiconductor component of the Van der Waals heterostructures under different strain

Strain	Lattice (Å)	n-type Schottky barrier (meV)	E_g (MoS ₂) (eV)
-1%	13.759	96	1.796
-0.5%	13.8285	50	1.74
0.0%	13.898	20	1.64
0.5%	13.9764	0	1.5
1%	14.037	-18	1.397

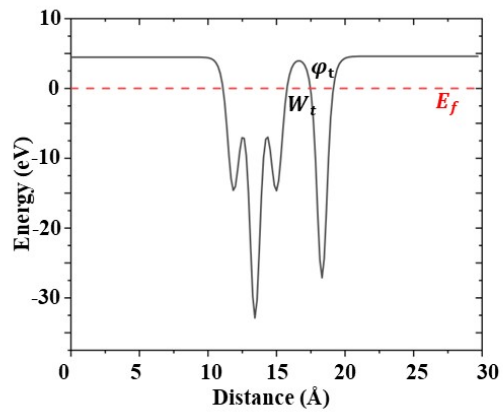


Fig. S3: (a) shows the electrostatic potential of the Graphene/MoS₂ heterostructure under the intrinsic condition, where φ_t is the tunneling height and W_t is the tunneling width.